Lattice distortion and magnetolattice coupling in CuO

Hiroshi Yamada[1,*] Xu-Guang Zheng,[2] Yuji Soejima,[1] and Masaru Kawaminami[3]
[1]*Department of Physics, Kyushu University, Fukuoka 812-8581, Japan*
[2]*Department of Physics, Saga University, Saga 840-8502, Japan*
[3]*Faculty of Science, Kagoshima University, Kagoshima, Japan*
(Received 24 February 2003; revised manuscript received 3 October 2003; published 17 March 2004)

High-resolution powder x-ray-diffraction measurements on cupric oxide CuO are carried out in an extensive temperature range from 100 K to 1000 K. Anomalies in the lattice constants appear at the known antiferromagnetic phase transitions at $T_{N1}=230$ K and $T_{N2}=213$ K, respectively, suggesting strong spin-lattice coupling in CuO. The Rietveld analysis with precise x-ray-diffraction data between 300 K and 1000 K clarifies a different structural phase transition at 800 K (T_S). Below 800 K, anisotropic behaviors in the Cu-Cu distances are observed along the $[10\bar{1}]$ and $[101]$ directions. The Cu-Cu distance along $[10\bar{1}]$ hardly changes in the temperature range below T_S, which is similar to the temperature dependence of the Cu-Cu distance in the CuO_2 plane of the high-T_C cuprate $La_{2-x}Sr_xCuO_4$. We suggest that the structural phase transition is caused by the softening of A_g^1 Raman mode at T_S. The present study elucidates a strong spin-lattice coupling in CuO below T_S, indicating persistence of magnetic interaction up to 3.5 times higher-temperature region than T_{N1}.

DOI: 10.1103/PhysRevB.69.104104 PACS number(s): 61.10.Nz, 61.50.Ks

I. INTRODUCTION

The role of copper-oxygen (Cu-O) bonds in the occurrence of superconductivity in Cu-based high-T_C superconductors (HTSC) has stimulated many reinspections on the physical properties of cupric oxide, CuO, since CuO is the simplest compound containing Cu-O covalent bonds. The magnetic properties, in particular, have been investigated in detail because it is believed that the magnetic coupling between $3d$ Cu^{2+} spins plays an important role for superconductivity in HTSC.[1,2] Heat-capacity[3–5] and neutron-scattering[6–8] measurements revealed two successive magnetic transitions; incommensurate antiferromagnetic (AF) phase between $T_{N1}=230$ K and $T_{N2}=213$ K, and commensurate AF phase below T_{N2}.[7–11] The AF transition, however, is extraordinary being compared with that in other monoxides of $3d$ transition metals such as MnO, FeO, CoO, and NiO: the magnetic susceptibility only shows a subtle change at T_{N1}, T_{N2},[4,12–16] and a broad maximum value around 540 K.[17] Another anomalous magnetic property is that the magnetic moment below T_{N2} is only 0.68 per Cu spin.[6,8] Although these features are explained by a quasi-one-dimensional spin system,[5,12,18,19] there are still a lot of controversy about the magnetic structure in CuO.

Recently, our group found different features in CuO: direct observation of charge ordering and charge stripes at ambient conditions,[20] which is the first report, to our knowledge, of an experimental evidence to show a link between CuO and HTSC. The charge ordering and charge stripes, together with alternated spin stripes, have previously been observed in HTSC, such as $La_{2-x}Sr_xCuO_4$, $YBa_2Cu_3O_{7-\delta}$, and $Bi_2Sr_2CaCu_2O_8$.[21–26] The alternated domain structures of charge stripes and spin stripes are considered to be intrinsic properties of HTSC. Furthermore, Bianconi *et al.* suggested that dynamic one-dimensional modulation with alternatively distorted and undistorted lattices exists in HTSC.[27–29] These results show that the charge, spin, and lattice in copper oxides strongly correlate to each other. Therefore, we think that the understanding of the correlation mechanism is very important for the study of superconductivity in HTSC. The discovery of charge stripes in CuO suggests that CuO is a model compound for studying charge-spin-lattice correlation. On the basis of this concept, we have extensively measured physical properties of CuO in a wide range of temperature including electric resistivity, magnetic susceptibility, dielectric constant, heat-capacity, electron-diffraction, and x-ray-diffraction measurements.[15,16,20,30–33] Another important result of these investigations is the finding of a different charge-spin-lattice coupled phase transition in CuO at 800 K: anomalies in the electric resistivity, magnetic susceptibility, and heat capacity in the vicinity of 800 K, and lattice distortion below 800 K (T_S) are observed. Except for our preliminary x-ray-diffraction studies, to our knowledge, no structural study on the temperature dependence of the crystal structure of CuO has been ever reported to date. The purpose of this work is to understand the phase transition through a detailed structural study. We have thus carried out synchrotron x-ray diffraction on CuO at temperatures ranging from 100 K to 1000 K. We demonstrate that strong magnetolattice correlation exists in CuO and that the lattice distortion at 800 K corresponds to a change of the local O^{2-} ionic coordination around Cu^{2+} ion, which is attributed to the softening of the A_g^1 Raman mode.

II. EXPERIMENTAL PROCEDURES AND DATA ANALYSIS

The present study was based on two independent experiments carried out at SPring-8, BL-02B2 (low-temperature measurement between 100 and 300 K, and high-temperature one between 300 and 1000 K, respectively). Powder samples were prepared by grinding high-quality single crystals, which were grown by the vapor-growth method.[30] This beam line is designed for the research of accurate structure analysis with powder samples and is able to collect high-angular resolution powder-diffraction data using a Debye-Scherrer cam-

TABLE I. Structural parameters of CuO refined by the Rietveld analysis at high temperatures. The crystal model for the refinements is space group $C2/c$ (No. 15), 4 Cu in $4(c)$: $(\frac{1}{4},\frac{1}{4},0;\frac{3}{4},\frac{3}{4},0;\frac{1}{4},\frac{3}{4},\frac{1}{2};\frac{3}{4},\frac{1}{4},\frac{1}{2})$, 4 O in $4(e)$: $(0,y,\frac{1}{4};\frac{1}{2},\frac{1}{2}+y,\frac{1}{4};0,\bar{y},\frac{3}{4};\frac{1}{2},\frac{1}{2}-y,\frac{3}{4})$.

T (K)	a (Å)	b (Å)	c (Å)	β (deg.)	V (Å^3)	y (O)	B (Cu)	B (O)	R_{WP}/R_{exp}
99.8	4.68457(11)	3.42219(9)	5.12887(12)	99.7037(9)	81.047(3)	0.4195(5)	0.19(1)	0.52(3)	3.35/1.36
119.2	4.68437(11)	3.42245(9)	5.12883(12)	99.6967(9)	81.051(3)	0.4199(6)	0.17(1)	0.39(4)	3.42/2.69
138.5	4.68422(11)	3.42257(9)	5.12867(13)	99.6893(9)	81.050(4)	0.4197(5)	0.19(1)	0.43(3)	3.48/2.68
157.9	4.68415(11)	3.42262(9)	5.12866(13)	99.6808(9)	81.052(4)	0.4213(5)	0.20(1)	0.46(3)	3.46/2.69
177.2	4.68428(11)	3.42264(9)	5.12871(13)	99.6712(9)	81.058(4)	0.4208(5)	0.22(1)	0.47(3)	3.37/2.69
196.6	4.68446(11)	3.42263(9)	5.12878(12)	99.6577(9)	81.065(3)	0.4217(5)	0.24(1)	0.52(3)	3.38/2.69
206.2	4.68450(11)	3.42255(9)	5.12866(12)	99.6497(9)	81.064(3)	0.4213(5)	0.28(1)	0.50(3)	3.29/2.69
215.9	4.68443(11)	3.42238(8)	5.12853(12)	99.6393(9)	81.059(3)	0.4215(5)	0.28(1)	0.47(3)	3.29/2.69
225.6	4.68448(11)	3.42209(9)	5.12844(12)	99.6261(9)	81.055(3)	0.4208(5)	0.30(1)	0.51(3)	3.27/2.69
235.2	4.68447(11)	3.42197(9)	5.12852(12)	99.6123(9)	81.056(3)	0.4210(5)	0.31(1)	0.55(3)	3.24/2.67
244.9	4.68443(11)	3.42202(9)	5.12853(13)	99.6000(9)	81.060(4)	0.4212(5)	0.32(1)	0.57(3)	3.22/2.68
273.9	4.68482(11)	3.42272(9)	5.12924(13)	99.5670(9)	81.103(4)	0.4215(5)	0.35(2)	0.62(3)	3.24/2.67
293.3	4.68552(11)	3.42374(9)	5.13023(13)	99.5451(9)	81.160(4)	0.4211(5)	0.41(2)	0.77(4)	3.17/1.34
400	4.6885(8)	3.4318(6)	5.1371(8)	99.419(5)	81.54(2)	0.425(2)	0.44(5)	2.67(23)	2.45/2.03
450	4.6911(8)	3.4348(5)	5.1398(8)	99.366(5)	81.71(2)	0.423(2)	0.40(4)	1.83(17)	4.02/0.94
500	4.6919(7)	3.4356(5)	5.1416(7)	99.310(4)	81.79(2)	0.427(2)	0.51(5)	2.24(19)	4.07/0.96
550	4.6938(8)	3.4372(5)	5.1439(8)	99.263(5)	81.91(2)	0.429(2)	0.63(5)	2.27(20)	3.94/1
600	4.6959(8)	3.4379(6)	5.1461(8)	99.219(5)	82.01(2)	0.430(2)	0.67(5)	2.65(21)	3.92/1.02
650	4.7005(4)	3.4399(3)	5.1499(4)	99.178(3)	82.21(1)	0.422(1)	0.79(4)	1.96(16)	2.64/1.61
700	4.7027(8)	3.4418(5)	5.1528(8)	99.112(5)	82.35(2)	0.427(2)	0.93(6)	2.40(23)	4.42/1.05
750	4.7053(6)	3.4430(4)	5.1549(7)	99.075(4)	82.47(2)	0.435(2)	0.69(5)	1.72(20)	3.71/1.24
800	4.7074(7)	3.4429(5)	5.1562(7)	99.054(4)	82.52(2)	0.437(2)	0.82(5)	1.86(20)	3.46/1.28
820	4.7093(7)	3.4436(4)	5.1579(7)	99.044(4)	82.61(2)	0.433(2)	0.92(6)	2.50(21)	3.33/1.32
840	4.7111(8)	3.4439(6)	5.1590(9)	99.035(5)	82.66(3)	0.427(2)	0.98(7)	3.05(27)	3.67/1.37
860	4.7131(7)	3.4442(5)	5.1601(7)	99.027(4)	82.73(2)	0.429(2)	1.06(6)	2.43(21)	3/1.39
870	4.7142(5)	3.4453(3)	5.1616(5)	99.042(3)	82.80(2)	0.426(1)	1.14(5)	2.32(17)	2.64/1.6
880	4.7148(7)	3.4448(5)	5.1618(7)	99.024(4)	82.80(2)	0.431(1)	1.09(6)	2.40(21)	2.96/1.42
900	4.7174(7)	3.4454(5)	5.1636(7)	99.018(4)	82.89(2)	0.430(2)	1.10(6)	2.41(21)	2.94/1.44
920	4.7197(6)	3.4449(4)	5.1647(7)	99.014(4)	82.94(2)	0.429(2)	1.20(6)	2.79(22)	2.88/1.46
940	4.7205(6)	3.4454(4)	5.1654(6)	99.012(4)	82.97(2)	0.430(2)	1.24(6)	2.67(21)	2.87/1.48
960	4.7216(6)	3.4461(4)	5.1664(7)	99.012(4)	83.03(2)	0.429(1)	1.27(6)	2.42(20)	2.84/1.48
999	4.7239(6)	3.4449(4)	5.1666(6)	99.006(3)	83.04(2)	0.429(2)	1.35(6)	2.61(21)	2.85/1.48

era with an imaging plate. The incident x-ray was monochromatized by a double crystal monochromator tuned to the wavelengths of 0.5 Å for both experiments. The temperature of the sample was controlled by a nitrogen gas flow cryostat in the low-temperature experiment, and a high-temperature gas flow system in the high-temperature measurement, respectively, with the temperature deviation within 1 K. Powder patterns at temperatures ranging from 100 K to 1000 K were collected over the 2θ range of $0°-68°$ in a step angle of 0.01°. All powder-diffraction data were analyzed by the Rietveld method, using the computer program RIETAN-2000.[34] For the refinements at each temperature, intensity data in the 2θ range of $8°-60°$ were used. The RIETAN-2000 has a choice over four kinds of peak profile functions and we finally selected the Toraya's split pseudo-Voigt function because of high flexibility as profile fitting.

The crystal structure of CuO at ambient condition was first investigated by Tunell *et al.*[35] and then, the structural parameters were refined by Åsbrink and Norrby.[36] The space group is $C2/c$ (No. 15) with Cu^{2+} ions occupying the symmetry site $4(c)$: $(\frac{1}{4},\frac{1}{4},0)$, $(\frac{3}{4},\frac{1}{4},\frac{1}{2})$, $(\frac{3}{4},\frac{3}{4},0)$, $(\frac{1}{4},\frac{3}{4},\frac{1}{2})$ and O^{2-} ions $4(e)$: $(0,y,\frac{1}{4})$, $(\frac{1}{2},\frac{1}{2}+y,\frac{1}{4})$, $(0,\bar{y},\frac{3}{4})$, $(\frac{1}{2},\frac{1}{2}-y,\frac{3}{4})$ with $y=0.4184$. The crystal symmetry did not change at the temperature range measured because the new appearance or the annihilation of peaks could not be observed in the powder patterns. The refinements of each powder pattern, finally, resulted in good values of the weighted R factor, R_{wp}, between 0.02 and 0.04 (see in Table I).

III. RESULTS

A. The temperature dependences of the lattice constants in the range of 100–300 K

The temperature dependences of the lattice constants a, b, c, β, and volume V at low temperatures are shown in Fig. 1 including the indicators of T_{N1} and T_{N2}. The crystal lattice changes corresponding to the magnetic phase transition are

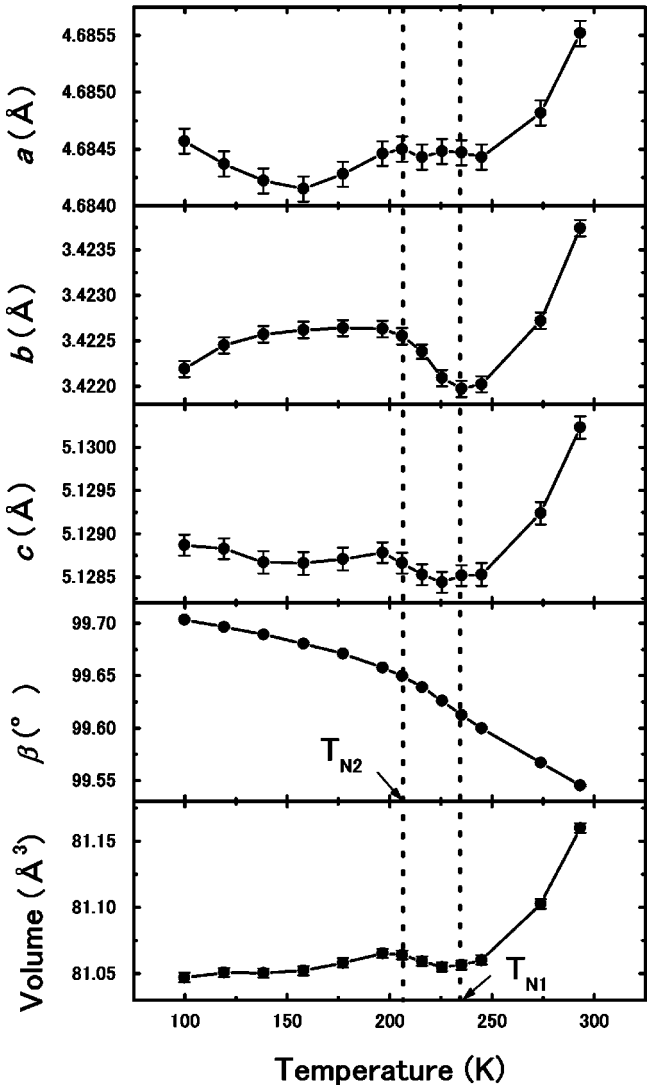

FIG. 1. The temperature dependences of the lattice constants at low temperatures.

clearly seen in these plots. First, the lattice constants except for β hardly change below T_{N1}, indicating the coupling of the spin ordering to the lattice. Second, all of the lattice constants show small changes in the temperature dependence at T_{N1} and T_{N2}.

Previously we have reported the signatures of the charge-spin-lattice coupling at the antiferromagnetic transitions T_{N1} and T_{N2} in dielectric constant measurements.[16,33] Recently further confirmation of this coupling has been made by the observation of abrupt steps on the temperature dependence curves of the thermal expansion coefficient.[37] Kuz'menko *et al.* also reported a spin-phonon coupling in CuO.[38] Therefore, we conclude that the lattice anomalies around T_{N1} and T_{N2} are a direct witness of the magnetolattice coupling. It is noted that there is a noticeable change in the temperature dependence of *a* around 150 K. In a previous report of Mössbauer-source experiment, an unusual temperature dependence of the electric quadrupole interaction near 150 K was indicated.[39] The present result clarifies that it is caused by a structural transformation.

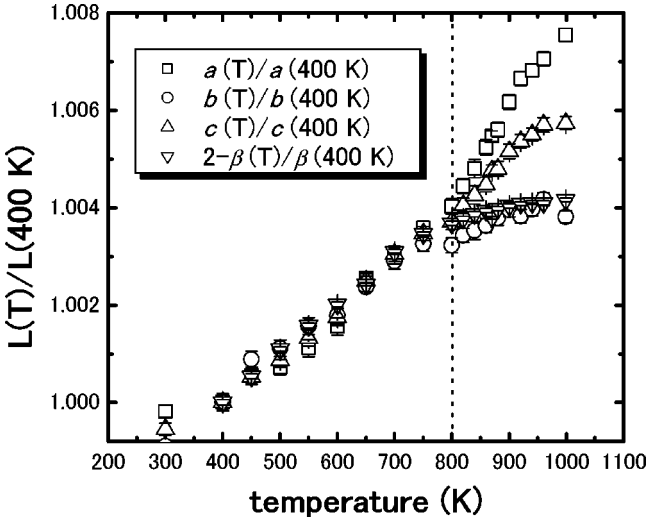

FIG. 2. The temperature dependences of the lattice constants. All data are normalized by the values at 400 K. About β, refer to the text. The temperature T_S, at which a charge-spin-lattice coupled phase transition was previously reported, is indicated by a broken line.

B. The temperature dependence of the lattice constants in the range of 300–1000 K

The unit cell of CuO is monoclinic with a lower symmetry than other 3*d* transition metal monooxides, which are all cubic. Therefore, it is considered that the extraordinary physical properties of CuO are probably caused by the lower symmetry and it is of interest to investigate the lattice distortion of CuO as a function of temperature. Shown in Table I are the lattice constants *a*, *b*, *c*, and β obtained from the Rietveld analysis at various temperatures. The temperature dependences are shown in Fig. 2 with each lattice constant normalized by the values at 400 K, respectively. β, however, was normalized by a formula $2-\beta/\beta(400\ \mathrm{K})$ because β has an inverse temperature dependence. The results qualitatively agree with the results of our preliminary experiments,[16] but show clearer changes at 800 K. All normalized lattice constants monotonously increase with increasing temperature at the same rate until 800 K, above which they show different temperature dependences. At temperatures higher than 800 K, *a* shows a rapid increase with increasing temperature, *c* shows the nearly same rate, while *b* and β show a much smaller temperature dependence. These imply that a structural instability like a structural phase transition occurs around 800 K. Actually, heat-capacity measurement using clean single crystals showed that a second-order-like phase transition occurs in the vicinity of this temperature.[16] Detailed analysis of the structural change at the transition revealed three specific features on the structure as are detailed below.

C. The intersecting and bending angles between two CuO ladders

The crystal structure of CuO, as shown in Fig. 3, consists of a stack of CuO ladders along $[110]$ and $[\bar{1}10]$ which

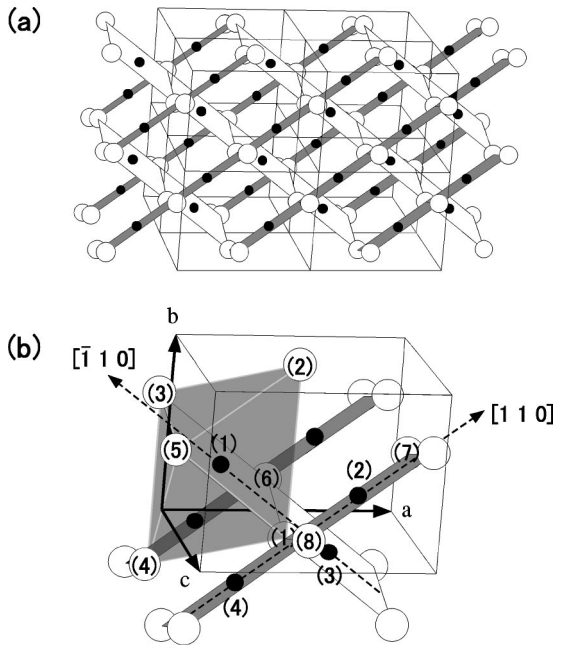

FIG. 3. The crystal structure of CuO. The four nearest-neighbor oxygen ions around a copper ion form a parallelogram. (a) Sharing the side of the parallelograms, two CuO ladders running along [110] and [$\bar{1}$10], respectively, are shown. (b) The oxygen ions around the copper ion can be also viewed as a distorted CuO_6 octahedral coordination, which is shown by the dim gray hatch. The copper and oxygen ions at different sites are denoted by the numbers in parentheses, which are used to indicate the distances and angle between ions.

intersect in the direction of [001] by sharing O^{2-} ions. The relation between the two ladders can be represented by the intersecting and bending angles θ_1 and θ_2: θ_1 is the angle between the running directions of the two ladders and θ_2 the angle between the parallelograms in each ladder. It should be noted that a statical precision of θ_1 is much better than that of θ_2 though the oxygen position shows comparatively a large uncertainty. This is because θ_1 has no relationship with the oxygen position, i.e., θ_1 can be directly estimated from the lattice constants a and b using the following formula: $\cos\theta_1=(b^2-a^2)/(a^2+b^2)$. As shown in Fig. 4, θ_1 and θ_2 show contrasting temperature dependences below and above 800 K; θ_1 becomes nearly temperature independent at lower temperatures, while θ_2 shows a maximum value at 800 K. It should be noted that on precision of the fitting parameters the errors of y axis of the O^{2-} ions are larger than those of other structural parameters, and therefore the error of θ_2 is larger than that of θ_1 because θ_1 is calculated only from lattice constants a, b.

D. The Cu-Cu distances

The change in the lattice constants is directly linked with the positional relation between Cu^{2+} ions, especially, it is interesting to investigate the Cu-Cu distances along the spin-ordering direction [10$\bar{1}$] and other directions. Shown in Fig. 5 are the Cu(1)-Cu(2) distance along [101] and Cu(3)-Cu(4) distance along [10$\bar{1}$]. The temperature dependence of the Cu-Cu distances abruptly changes at 800 K. At $T>800$ K, the temperature dependence is actually identical for the two directions, while it is anisotropic at $T<800$ K. The Cu(3)-Cu(4) distance along the [10$\bar{1}$] direction turns to become almost constant at $T<800$ K, while the Cu(1)-Cu(2) distance continues to decrease monotonically with decreasing temperature.

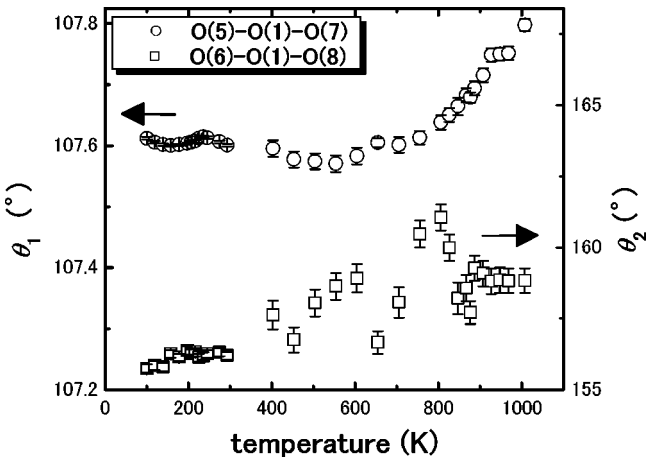

FIG. 4. The temperature dependences of the intersecting angle θ_1 and the bending angle θ_2, which correspond to the angles of O(5)-O(1)-O(7) and O(6)-O(1)-O(8), respectively. The oxygen positions are indicated by the numbers in parentheses according to Fig. 3(b).

E. The O^{2-} ion coordination around Cu^{2+} ion

Another structural view of CuO can be drawn by considering that the four nearest-neighbor O^{2-} ions and two next nearest O^{2-} ions (which are on the intersecting Cu-O ladder) around a Cu^{2+} ion form a strongly distorted octahedral (4 +2) coordination as shown in Fig. 3(b) by the gray section. Remarkable changes can be observed in the octahedral coordination below and above 800 K. The temperature depen-

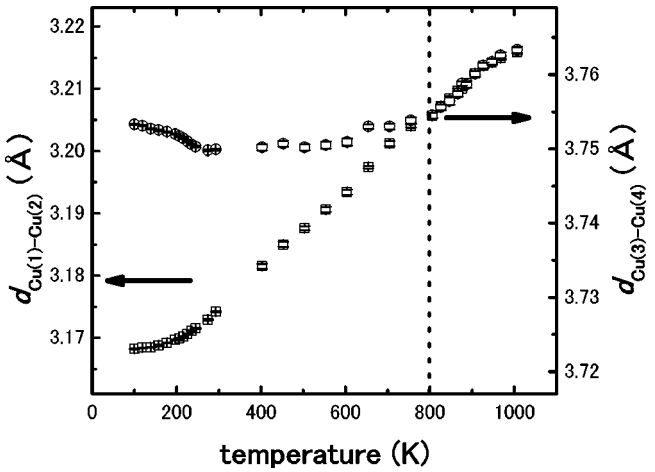

FIG. 5. The temperature dependences of the Cu-Cu distances. Numbers in parentheses are according to Fig. 3(b). T_S is indicated by a broken line.

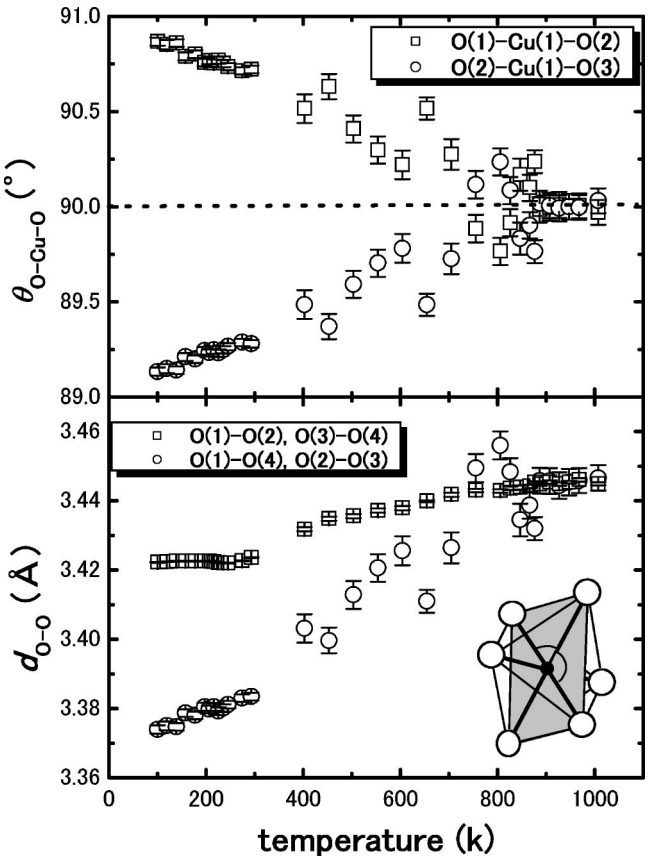

FIG. 6. The temperature dependences of the O-O distances and the O-Cu-O angles in the distorted CuO_6 octahedron shown in Fig. 3(b). The numbers in parentheses are according to Fig. 3(b). The copper and oxygen coordination is indicated in the inset.

dences of the O-O distances and O-Cu-O bond angles are shown in Fig. 6. The O-O distances in the parallelogram become identical and the O-Cu-O angles become 90° when the temperature exceeds 800 K, i.e., the coordination change from a parallelogram to a lozenge. This means that the ligand field around the Cu^{2+} ion takes a high symmetry above 800 K.

IV. DISCUSSION

The powder synchrotron x-ray-diffraction measurements of CuO clearly show that a structural change occurs at $T_S = 800$ K. Since anomalous behaviors around T_S have been observed in the electrical resistivity, magnetic susceptibility, and specific-heat measurements with high-quality single crystals,[16] it is reasonable to think that the structural change correlates with electrons and spins. The change is characterized by three structural features: (a) the change of the intersecting and bending angles between CuO ladders, (b) the anisotropic temperature dependences of Cu-Cu distances, and (c) the change of the local symmetry in O^{2-} ions coordination around Cu^{2+} ion. First, about the change of the intersecting and bending angles, it is reasonable to consider possible vibration modes in CuO. The primitive unit cell of CuO contains two molecular units and thus there are 12 vibration modes. Since the Cu ions are located on sites with C_i symmetry and the O ions on sites with C_2 symmetry, it is possible to yield the vibration modes[40–42] $(q=0)$

$$\Gamma = 4Au + 5Bu + Ag + 2Bg,$$

where $Au+2Bu$ are three acoustic modes, the six $3Au+3Bu$ modes infrared active, and the three $Ag+2Bg$ modes Raman active. The ion displacements of the Raman active mode are shown in Fig. 7. It should be noted that Cu^{2+} ions are stabilized at symmetry sites and only O^{2-} ions are displaced. The Ag Raman mode indicates displacements of O^{2-} ions along the b axis and corresponds to the interladder bending mode. Since the bending angle θ_2 decreases with decreasing temperature below T_S, it is implied that the Ag mode softens at T_S. In these measurements, as mentioned above, we could not get sufficient precision on positional determination of O^{2-} ions. Recently, Yashima has repeated the investigation by neutron powder diffraction at high temperatures, and confirmed that the fractional coordinates y of O^{2-} ion is stable above T_S and decreases monotonously with cooling below T_S.[43] Their results are qualitatively in agree-

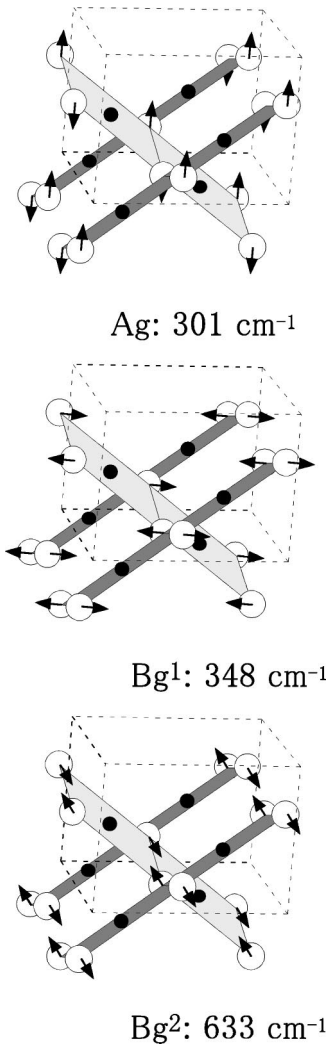

FIG. 7. Raman mode displacements of CuO. The values of experimental phonon frequencies by Kliche and Popovic (see Ref. 47) are given.

ment with the present results, but the value of y is relatively smaller. The subtle discrepancy is explained by the difference in the ability to determine the oxygen position between neutron and x-ray diffraction. The softening of the A_g^1 mode can be verified by the investigation on the lattice dynamics in CuO. Unfortunately Raman- and infrared-scattering measurements at high temperatures have not been done.

Second, the anisotropic feature of the Cu-Cu distances is probably correlated with the magnetic properties in CuO. The inelastic neutron-scattering measurements by Aïn *et al.*[44] demonstrated that the exchange interactions between Cu^{2+} ions are strongly anisotropic: $J(10\bar{1})=80$ meV, $J(101)=5$ meV, $J(010)=3$ meV. Reflecting the anisotropic magnetic interaction, one-dimensional antiferromagnetic spin ordering along $[10\bar{1}]$ occurs as a long range below T_{N1}, and strong anisotropic magnetic correlations and fluctuation are observed well above T_{N1}.[8,19] These properties are clues to explain the extraordinary behavior of magnetic susceptibility in CuO: it does not show the usual Curie-Weiss dependence above T_{N1} but a broad maximum around 550 K. Therefore, it can be considered that the anisotropic behavior of the Cu-Cu distances below 800 K is correlated with the anisotropy of Cu-Cu interaction. A supporting evidence about the correlation of the lattice changes and magnetic coupling comes from our experiment on Li-doped CuO.[45] Substitution of Cu by Li considerably decreases T_{N1} and T_{N2}. Meanwhile, a-axis length, β, and the Cu-Cu distance along the $[10\bar{1}]$ increase with Li substitution. The structural change due to Li substitution strikingly resembles that of pure CuO at $T>800$ K. According to the previous electrical, magnetic, and heat-capacity measurements that we carried out with single crystal CuO,[16] it is natural to conclude that the structural changes above T_s are a result of charge excitation and diminishing of Cu^{2+} spins, which are suspected to be due to hole excitation from oxygen to copper site. Therefore, we conclude that the magnetic correlation in CuO exists until 800 K. It should be noted that the structural change at 800 K is similar to the structural phase transition of the HTSC's $La_{2-x}Sr_xCuO_4$ (LSCO), in which a structural phase transition from tetragonal to orthorhombic phase occurs. Due to this phase transition, the CuO_2 plane distorts from square to rectangle and causes buckling in the CuO_2 two-dimensional planes, which plays an important role for the superconductivity. The change in the bending angle between the CuO_2 ladders in CuO may be similar to the buckling of the CuO_2 plane in LSCO. Furthermore, it is surprising that the Cu-Cu distances in CuO_2 plane of LSCO is nearly temperature independent in the orthorhombic phase,[46] which is same as those of CuO below T_S. These facts also indicate that the structural instability, especially the displacement of O^{2+} ions, is essential for copper oxide consisting of Cu-O units.

Finally, it is interesting to note the change in O^{2-} ion coordination around Cu^{2+} ion at 800 K. The parallelogram shown in Fig. 6 forms a plane perpendicular to $[10\bar{1}]$ by sharing all sides. Since large spin interaction exists in Cu-O-Cu zigzag chains along $[10\bar{1}]$ and the Cu-Cu distance in this direction does not change below 800 K, it seems that the symmetry change of the ligand field around Cu^{2+} ion causes the change of interaction between Cu^{2+} spins.

V. CONCLUSION

Powder x-ray-diffraction experiments of CuO in an extensive temperature range have been carried out with synchrotron x-ray, and the structural change as a function of temperature has been investigated in detail by the Rietveld analysis. Minor changes in the crystal structure are found at the known antiferromagnetic transition at T_{N1} and T_{N2}, demonstrating the coupling of the lattice to the magnetic ordering. A structural phase transition at $T_S=800$ K is clarified. Remarkable lattice changes at T_S are characterized by three structural features as summarized below.

(1) The intersecting and bending angles between the CuO ladders running along $[110]$ and $[\bar{1}10]$ show contrasting temperature dependences; the decrease of the bending angle below T_S can be explained by the softening of the A_g Raman mode.

(2) Anisotropic temperature dependences of Cu-Cu distances appear below T_S; the Cu-Cu distances along the antiferromagnetic spin-ordering direction is almost temperature independent similar to that observed in $La_{2-x}Sr_xCuO_4$ ($x\sim0.143$).

(3) The symmetry of O^{2-} ion's coordination in the distorted CuO_6 octahedron slightly changes at T_S. This feature corresponds to the change of the crystal field, and implies the change of the electronic state of $3d$ electrons in Cu^{2+} ion.

This explains the previously reported electric and magnetic anomalies at 800 K.[16] The present study supports our previous indication of strong spin-lattice coupling, and suggests that magnetic interaction in CuO persists until $T_S=800$ K at which a transition to a higher crystal symmetry occurs. This study also suggests that lattice distortion might be an essential property of copper oxides containing Cu-O bonds. Infrared and Raman experiments at high temperatures are demanded to study the structural instability at T_S in detail.

ACKNOWLEDGMENTS

The authors thank A. Okazaki for useful discussion. This work was partly supported by The Venture Business Laboratory in Kyushu University, and Japan Science and Technology Corporation.

*Corresponding author. Electronic address: hiro-yamada@aist.go.jp

[1] A.J. Millis, H. Monien, and D. Pines, Phys. Rev. B **42**, 167 (1990).
[2] P. Monthoux, A.V. Balatsky, and D. Pines, Phys. Rev. B **46**, 14 803 (1992).
[3] R.W. Millar, J. Am. Chem. Soc. **51**, 215 (1929).
[4] M.S. Seehra, Z. Feng, and R. Gopalakrishnan, J. Phys. C **21** (1988).
[5] J.W. Loram, K.A. Mirza, C.P. Joyce, and A.J. Osborne, Europhys.

Lett. **8**, 263 (1989).
[6] B.N. Brockhouse, Phys. Rev. **94**, 781 (1954).
[7] B.X. Yang, J.M. Tranquada, and G. Shirane, Phys. Rev. B **38**, 174 (1988).
[8] B.X. Yang, T.R. Thurston, J.M. Tranquada, and G. Shirane, Phys. Rev. B **39**, 4343 (1989).
[9] J.B. Forsyth, P.J. Brown, and B.M. Wanklyn, J. Phys. C **21**, 2917 (1988).
[10] P.J. Brown, T. Chattopadhyay, J.B. Forsyth, V. Nunez, and F. Tasset, J. Phys.: Condens. Matter **3**, 4281 (1991).
[11] M. Aïn, A. Menelle, B.M. Wanklyn, and E.F. Bertaut, J. Phys.: Condens. Matter **4**, 5327 (1992).
[12] O. Kondo, M. Ono, E. Sugiura, K. Sugiyama, and M. Date, J. Phys. Soc. Jpn. **57**, 3293 (1988).
[13] U. Köbler and T. Chattopadhyay, Z. Phys. B: Condens. Matter **82**, 383 (1991).
[14] D.D. Lawrie, J.P. Franck, and C.-T. Lin, Physica C **297**, 59 (1998).
[15] X.G. Zheng, N. Tsutsumi, S. Tanaka, M. Suzuki, and C.N. Xu, Physica C **321**, 67 (1999).
[16] X.G. Zheng, C.N. Xu, E. Tanaka, Y. Tomokiyo, H. Yamada, Y. Soejima, Y. Yamamura, and T. Tsuji, J. Phys. Soc. Jpn. **70**, 1054 (2001).
[17] M. O'keeffe and F.S. Stone, J. Phys. Chem. Solids **23**, 261 (1962).
[18] K. Kondo, M. Honda, T. Kohashi, and M. Date, J. Phys. Soc. Jpn. **59**, 2332 (1990).
[19] T. Chattopadhyay, G.J. McIntyre, P.J. Brown, and J.B. Forsyth, Physica C **170**, 371 (1990).
[20] X.G. Zheng, C.N. Xu, Y. Tomokiyo, E. Tanaka, H. Yamada, and Y. Soejima, Phys. Rev. Lett. **85**, 5170 (2000).
[21] J.M. Tranquada, B.J. Stemlieb, J.D. Axe, U. Nakamura, and S. Uchida, Nature (London) **375**, 561 (1995).
[22] J.M. Tranquada *et al.*, Phys. Rev. B **54**, 7489 (1996).
[23] J.M. Tranquada *et al.*, Phys. Rev. Lett. **78**, 338 (1997).
[24] T. Noda, H. Eidaki, and S.-I. Uchida, Science **286**, 265 (1999).
[25] X.J. Zhou, P. Bogdanov, S.A. Kellar, T. Noda, H. Eisaki, S. Uchida, Z. Hussain, and Z.-X. Shen, Science **286**, 268 (1999).
[26] H.A. Mook *et al.*, Nature (London) **395**, 580 (1998).
[27] A. Bianconi, Solid State Commun. **89**, 933 (1994).
[28] A. Bianconi and M. Missori, Solid State Commun. **91**, 287 (1994).
[29] A. Bianconi, N.L. Saini, A. Lanzara, M. Missori, T. Rossetti, H. Oyanagi, H. Yamaguchi, K. Oka, and T. Ito, Phys. Rev. Lett. **76**, 3412 (1996).
[30] X.G. Zheng *et al.*, Mater. Res. Bull. **33**, 605 (1998).
[31] X.G. Zheng *et al.*, J. Therm Anal. Calorim. **57**, 853 (1999).
[32] X.G. Zheng *et al.*, Philos. Mag. Lett. **79**, 819 (1999).
[33] X.G. Zheng, Y. Sakurai, Y. Okayama, T.Q. Yang, L.Y. Zhang, X. Yao, K. Nonaka, and C.N. Xu, J. Appl. Phys. **92**, 2703 (2002).
[34] F. Izumi and T. Ikeda, Mater. Sci. Forum **321-324**, 198 (2000).
[35] G. Tunell, E. Posnjak, and C.J. Ksanda, Z. Kristallogr. **90**, 120 (1935).
[36] S. Asbrink and L.-J. Norrby, Acta Crystallogr., Sect. B: Struct. Crystallogr. Cryst. Chem. **26**, 8 (1970).
[37] M. Ohashi (private communication).
[38] A.B. Kuz'menko, D. van der Marel, P.J.M. van Bentum, E.A. Tishchenko, C. Presura, and A.A. Bush, Phys. Rev. B **63**, 094303 (2001).
[39] C. Niedermayer *et al.*, Phys. Rev. B **38**, 2836 (1988).
[40] J.C. Irwin, J. Chrzanowski, and T. Wei, Physica C **166**, 456 (1990).
[41] J. Chrzanowski and J.C. Irwin, Solid State Commun. **70**, 11 (1989).
[42] C.C. Homes, M. Ziaei, B.P. Clayman, J.C. Irwin, and J.P. Franck, Phys. Rev. B **51**, 3140 (1995).
[43] M. Yashima (private communication).
[44] M. Aïn, W. Reichardt, B. Hennion, G. Pepy, and B.M. Wanklyn, Physica C **162-164**, 1279 (1989).
[45] X.G. Zheng, H. Yamada, D.J. Scanderbeg, M.B. Maple, and C.N. Xu, Phys. Rev. B **67**, 214516 (2003).
[46] H. Yamada, Ph.D. thesis, Kyushu University, 1997.
[47] G. Kliche and Z.V. Popovic, Phys. Rev. B **42**, 10060 (1990).